tion is likely to destroy actin binding of *Myo15*, creating a loss-of-function allele. *Myo15* led to identification of the human homolog, *MYO15*, and to the discovery of a nonsense mutation and two missense mutations in three unrelated human families with nonsyndromic, congenital deafness, *DFNB3* (9).

Mutations in three different unconventional myosins, $Myo15^{sh2}$, $Myo6^{sv}$, and $Myo7a^{sh1}$, cause deafness (13). Morphology and histology of severe loss-of-function alleles in the mouse suggest that each of these myosins has a unique function in the hair cells of the inner ear. Our results show that *Myo15* is involved in the maintenance of actin organization in the hair cells of the organ of Corti. Loss of *Myo7a* causes disorganization of the characteristic pattern of the stereocilia early in development, whereas loss of *Myo6* function causes fusion of the stereocilia and loss of the inner hair cells and support cells by 6 weeks of age (14). In contrast, the inner hair cells of *sh2* mutants survive longer (15) and the abnormally short stereocilia are arranged in a nearly normal pattern on the hair cell surface. These features make *shaker-2* mice a good model for examining the role of a unique unconventional myosin in the auditory system and for the exploration of mechanisms for the delivery of functional proteins to surviving mutant hair cells.

REFERENCES AND NOTES

1. N. Dobrovolskaia-Zavasdkaia, *Arch. Biol.* **38**, 457 (1928); G. D. Snell and L. W. Law, *J. Hered.* **30**, 447 (1939).
2. T. B. Friedman *et al.*, *Nature Genet.* **9**, 86 (1995).
3. Y. Liang *et al.*, *Am. J. Hum. Genet.* **62**, 904 (1998).
4. A. Sobin and A. Flock, *Adv. Oto-Rhino-Laryngol.* **25**, 12 (1981); D. Kohrman, E. Lambert, D. V. Garrett, D. F. Dolan, Y. Raphael, paper presented at the 21st Midwinter Research Meeting of the Association for Research in Otolaryngology, St. Petersburg Beach, FL, 1998 (www.aro.org); A. Sobin, M. Anniko, A. Flock, *Arch. Oto-Rhino-Laryngol.* **236**, 1 (1982).
5. Y. Wakabayashi *et al.*, *Biochem. Biophys. Res. Commun.* **234**, 107 (1997); F. Probst, Q. Xhao, K.-S. Chen, A. Wang, T. Friedman, J. Lupski, S. Camper, unpublished data.
6. R. K. Wilson and E. R. Mardis, in *Analyzing DNA*, B. Birren, E. D. Green, S. Klapholz, R. M. Myers, J. Roskams, Eds. (Cold Spring Harbor Laboratory Press, Cold Spring Harbor, NY, 1997), p. 398; S. F. Altschul, W. Gish, W. Miller, E. W. Myers, D. J. Lipman, *J. Mol. Biol.* **215**, 403 (1990). SeqWright Inc. (Houston, TX) generated the M13 DNA shotgun library and approximately half of the sequence data. Sequence contig assembly and editing were performed with the Sequencher program (Gene Codes Corp., Ann Arbor, MI); the web sites for GRAIL and GENSCAN are http://compbio.ornl.gov/Grail-bin/EmptyGrailForm and http://gnomic.stanford.edu/~chris/GENSCANW.html [C. Burge and S. Karlin, *J. Mol. Biol.* **268**, 78 (1997)].
7. V. Mermall, P. L. Post, M. S. Mooseker, *Science* **279**, 527 (1998).
8. P. Linder, *Nature* **337**, 121 (1989); the consensus ATP-GTP binding site is (A/G)XXXXGK(S/T/G) and the *Myo15* sequences are GESDSGKT, amino acids 132 to 139, and APPRLGKS at amino acids 566 to 573 (16). The *Myo15* cDNA sequence has been deposited in GenBank (accession number AF053130).
9. A. Wang *et al.*, *Science* **280**, 1447 (1998).
10. F. J. Probst, R. A. Fridell, Y. Raphael, T. L. Saunders, A. Wang, Y. Liang, R. J. Morell, J. W. Touchman, R. H. Lyons, K. Noben-Trauth, T. B. Friedman, S. A. Camper, data not shown.
11. Myosin home page, Medical Research Council, UK (www.mrc-lmb.cam.ac.uk/myosin/myosin.html).
12. H. M. Warrick and J. A. Spudich, *Annu. Rev. Cell. Biol.* **3**, 379 (1987); J. A. Porter and C. Montell, *J. Cell Biol.* **122**, 601 (1993).
13. K. A. Avraham *et al.*, *Nature Genet.* **11**, 369 (1995); F. Gibson *et al.*, *Nature* **374**, 62 (1995); D. Weil *et al.*, *ibid.*, p. 60; X. Liu *et al.*, *Nature Genet.* **16**, 188 (1997); D. Weil *et al.*, *ibid.*, p. 191; C. Petit, *ibid.* **14**, 385 (1996).
14. T. Self *et al.*, *Development* **125**, 557 (1998); K. Steel and K. Avraham, personal communication.
15. M. S. Deol, *J. Genet.* **52**, 562 (1954).
16. Abbreviations for the amino acid residues are as follows: A, Ala; C, Cys; D, Asp; E, Glu; F, Phe; G, Gly; H, His; I, Ile; K, Lys; L, Leu; M, Met; N, Asn; P, Pro; Q, Gln; R, Arg; S, Ser; T, Thr; V, Val; W, Trp; and Y, Tyr.
17. Y. Raphael and R. A. Altschuler, *Cell Motil. Cytoskeleton* **18**, 215 (1991); Y. Raphael, B. Athey, Y. Wang, M. K. Lee, R. A. Altschuler, *Hear. Res.* **76**, 173 (1994).
18. W. F. Dietrich *et al.*, *Nature Genet.* **7**, 220 (1994).
19. B. Hogan, R. Beddington, F. Costantini, E. Lacey, *Manipulating the Mouse Embryo: A Laboratory Manual* (Cold Spring Harbor Laboratory Press, Cold Spring Harbor, NY, 1994).
20. J. D. Thompson, D. G. Higgins, T. J. Gibson, *Nucleic Acids Res.* **22**, 4673 (1994); PHYLIP package, J. Felsenstein, University of Washington.

21. All experiments involving animals were approved by the University of Michigan Committee on the Use and Care of Animals. Animals were housed in facilities accredited by the American Association for the Accreditation of Laboratory Animal Care. The university's Animal Welfare Assurance is on file with the NIH Office for Protection from Research Risks (A3114-01). All procedures are in compliance with guidelines and standards set by local, state, and federal agencies. Supported by NIDCD intramural research projects Z01 DC 00035, Z01 DC 00038, and Z01 DC 02407 (T.B.F.), and extramural grant R01DC 01634 (Y.R.), National Institute of Child Health and Human Development grant R01 HD30428 (S.A.C.), NSF (F.J.P.), and National Institute of General Medical Sciences grant T32 GM07863 (F.J.P.). We thank N. Dietrich, M. Fergusson, A. Gupta, E. Sorbello, R. Torkzadeh, C. Varner, M. Walker, G. Bouffard, and S. Beckstrom-Sternberg of the NIH Intramural Sequencing Center; C. Esposito, S. Genik, A. Thomas, and H. Luderer of the University of Michigan DNA Sequencing Core; P. Gillespie and M. Berard of the University of Michigan Transgenic Animal Model Core; L. Beyer, D. Dolan, K. Douglas, C. Edwards, E. Lambert, G. Levy, and P. Tucker of the University of Michigan; and J. Beals of PhotoGraphic for their contributions.

9 March 1998; accepted 17 April 1998

Association of Unconventional Myosin *MYO15* Mutations with Human Nonsyndromic Deafness *DFNB3*

Aihui Wang, Yong Liang, Robert A. Fridell, Frank J. Probst, Edward R. Wilcox, Jeffrey W. Touchman, Cynthia C. Morton, Robert J. Morell, Konrad Noben-Trauth, Sally A. Camper, Thomas B. Friedman*

DFNB3, a locus for nonsyndromic sensorineural recessive deafness, maps to a 3-centimorgan interval on human chromosome 17p11.2, a region that shows conserved synteny with mouse *shaker-2*. A human unconventional myosin gene, *MYO15*, was identified by combining functional and positional cloning approaches in searching for *shaker-2* and *DFNB3*. *MYO15* has at least 50 exons spanning 36 kilobases. Sequence analyses of these exons in affected individuals from three unrelated *DFNB3* families revealed two missense mutations and one nonsense mutation that cosegregated with congenital recessive deafness.

Nonsyndromic recessive deafness accounts for about 80% of hereditary hearing loss (1). To date, 20 loci responsible for this form of deafness have been mapped and three have been identified (2–4). *DFNB3*, first identified in families from Bengkala, Bali, initially was mapped to a 12-centimorgan (cM) region near the centromere of chromosome 17 (5) and subsequently was refined to a 3-cM region of 17p11.2 (6). Congenital hereditary deafness in two unrelated consanguineous families from India is also linked to *DFNB3* (6), indicating that the contribution of *DFNB3* alleles to hereditary deafness is likely to be geographically widespread.

On the basis of conserved synteny and similar phenotypes, we proposed that the autosomal recessive mouse mutation *shaker-2* was the homolog of *DFNB3* (5, 6). In the accompanying paper, we describe the bacterial artificial chromosome (BAC)–mediated transgene correction of the deafness and circling phenotype of homozygous *shaker-2* mice (7). DNA sequence analyses of this BAC revealed an unconventional myosin gene, *Myo15*. Myosins are a family of actin-based molecular motors that use energy from hydrolysis of adenosine triphosphate (ATP) to generate mechanical force. The classic, two-headed filament-forming myosins that provide the basis for muscle contraction are referred to as conventional myosins. Other members of the myosin superfamily, the unconventional myosins,

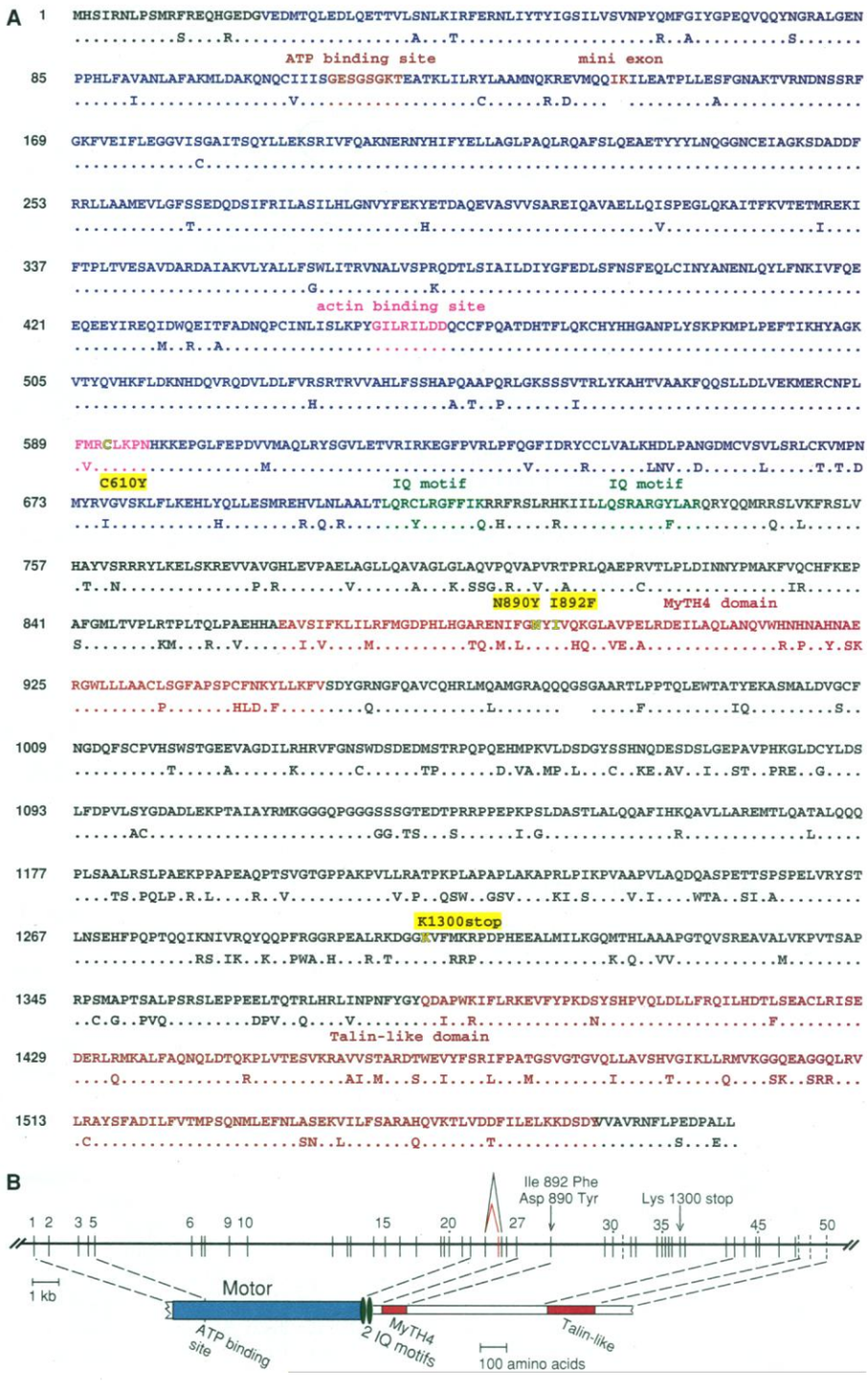

Fig. 1. (**A**) Predicted amino acid sequence of *MYO15*. A partial *MYO15* cDNA (4757 bp) is predicted to encode 1585 amino acids with a motor domain (blue), two IQ motifs (green), and a tail region containing a MyTH4 and a talin-like domain (red). A consensus ATP binding site and two putative actin binding sites within the motor domain are indicated (red and pink, respectively). Mini-exon 6 in the motor domain is also shown (red). The corresponding mouse Myo15 sequence is shown below the human sequence. Amino acid identities are indicated by dots. The three *DFNB3* mutations (N890Y, I892F, and K1300X) are highlighted in yellow above the sequence, and the *shaker-2* mutation (C610Y) is highlighted in yellow below the sequence. (**B**) Genomic structure of *MYO15*. Relative positions of 50 *MYO15* exons in 35.9 kb of genomic DNA sequence are indicated. Intronic sequences are drawn to scale but exons are not. Solid black or red vertical lines represent exons that have been identified in cDNA clones. Dashed vertical lines represent exons that are predicted based on GENSCAN, GRAIL, and conservation between human and mouse sequences. Alternative exon 24 (red vertical line) was found in a brain cDNA clone. Exon 24 has stop codons in all three reading frames and, if included in a transcript, would result in a MYO15 isoform with a shorter tail. The three *DFNB3* mutations and the domain organization of the encoded MYO15 protein are also shown.

have functions that are less well understood but in some cases are thought to mediate intracellular trafficking events (*8*). All myosins share a common structural organization consisting of a conserved NH_2-terminal motor domain followed by a variable number of light-chain binding (IQ) motifs and a highly divergent tail. In the *shaker-2* mouse, an amino acid substitution was found in a conserved residue in the motor domain of Myo15 (*7*). Here we report the identification of human *MYO15* (*9*) and describe three mutations of this gene that cause hereditary deafness in three *DFNB3* families (*10*).

To isolate *MYO15*, we used primers to predict exons of the mouse homolog to amplify human genomic DNA. Sequence analyses of four polymerase chain reaction (PCR) products showed 99% identity to *Myo15* at the amino acid level (*11*), indicating that the isolated PCR products were derived from *MYO15*. When these human sequences were used as starting points, a partial *MYO15* cDNA sequence of ~2.3 kilobases (kb) was identified by RACE (rapid amplification of cDNA ends) and reverse transcription–PCR (RT-PCR) (*12*). To obtain additional *MYO15* sequences, we isolated genomic clones from a human chromosome 17–specific cosmid library, and the 35.9-kb insert from one clone was completely sequenced (*13*) (GenBank accession number AF051976). Coding regions were identified by means of gene structure

A. Wang and Y. Liang, Laboratory of Molecular Genetics, National Institute on Deafness and Other Communication Disorders, National Institutes of Health, Rockville, MD 20850, USA, and Graduate Program in Genetics, Michigan State University, East Lansing, MI 48824, USA.
R. A. Fridell, E. R. Wilcox, K. Noben-Trauth, R. J. Morell, T. B. Friedman, Laboratory of Molecular Genetics, National Institute on Deafness and Other Communication Disorders, National Institutes of Health, Rockville, MD 20850, USA.
F. J. Probst and S. A. Camper, Department of Human Genetics, University of Michigan, Ann Arbor, MI 48109, USA.
J. W. Touchman, NIH Intramural Sequencing Center, National Institutes of Health, Rockville, MD 20850, USA; National Human Genome Research Institute, National Institutes of Health, Bethesda, MD 20892, USA.
C. C. Morton, Departments of Pathology, Obstetrics, Gynecology and Reproductive Biology, Brigham and Women's Hospital and Harvard Medical School, Boston, MA 02115, USA.

*To whom correspondence should be addressed. E-mail: tfriedman@pop.nidcd.nih.gov

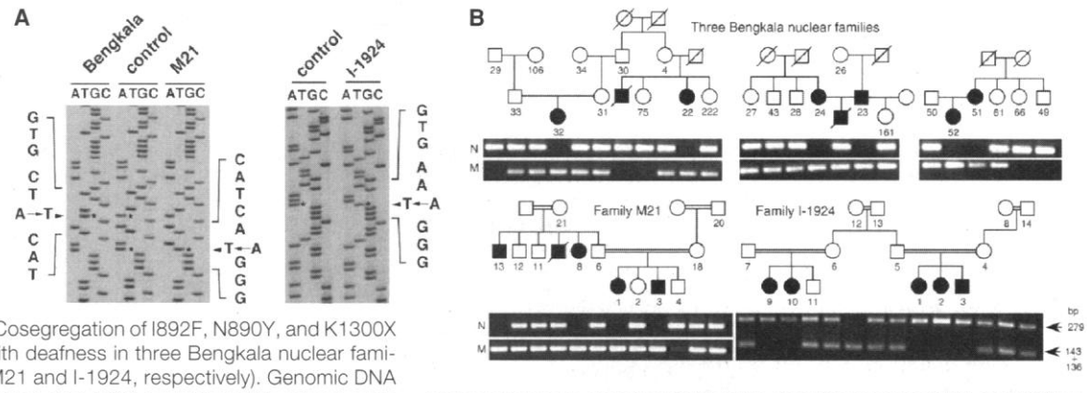

Fig. 2. (**A**) *MYO15* mutations in the Bengkala kindred and two unrelated Indian families, M21 and I-1924. Portions of *MYO15* DNA sequences are shown for an individual with normal hearing (control) and for an affected individual from each of the three *DFNB3* families. The position of each mutation and the corresponding normal allele is indicated by an arrow and an asterisk. (**B**) Cosegregation of I892F, N890Y, and K1300X point mutations of *MYO15* with deafness in three Bengkala nuclear families and two Indian families (M21 and I-1924, respectively). Genomic DNA from individuals in these families was PCR amplified with primer pairs specific for normal (N) or mutant (M) alleles (*31*). Amplification products in each lane correspond to numbered individuals directly above in the pedigrees. In each family, all deaf individuals are homozygous for the mutant *MYO15* allele. Their hearing parents are heterozygotes. Cosegregation of the mutant allele with deafness in the second Indian family I-1924 was demonstrated by RFLP analysis. Genomic NA was PCR amplified and digested with Xmn I. PCR products obtained from the normal alleles are digested ith Xmn I to yield fragments of 143 and 136 bp, whereas PCR products from the mutant alleles are not digested, yielding a 279-bp fragment only. All deaf individuals in family I-1924 are homozygous for the mutant allele and show the 279-bp fragment only. Obligate carriers have Xmn I-digested and undigested fragments. Each member of the three *DFNB3* families gave consent to publish unaltered family relationships, which are excerpted from the complete pedigrees published elsewhere (*6*).

prediction programs (*14*), homology search (BLASTX) (*15*), and Pustell DNA matrix analysis (MacVector 6.0) (*16*), which together predicted the presence of 49 exons in this cosmid. Of these, 45 *MYO15* exons have thus far been identified in cDNA clones (*12*, *17*). A 6-base pair (bp) exon 6 was not predicted but is present in a *MYO15* cDNA clone (*18*). The longest *MYO15* open reading frame deduced from the overlapping cDNAs is 4757 bp, which comprises 45 exons (Fig. 1A) (*19*).

To determine whether *MYO15* maps to the *DFNB3* critical region, we used a primer pair derived from *MYO15* intron 15 to amplify DNA from somatic cell hybrid lines containing various deletions of chromosomal region 17p11.2 (6). The results demonstrated that *MYO15* maps to the 3-cM *DFNB3* critical region (*20*).

Searches of public nucleotide and protein databases with the *MYO15* cDNA sequence (4757 bp) revealed no exact matches, and the highest significant matches were to actual or predicted unconventional myosins (*21*). In MYO15, a motor domain from codon 21 to 696 was identified by alignment against chicken skeletal muscle myosin II (GgFSK) (Fig. 1, A and B) (*22*). Alignments with other myosins reveal a consensus ATP binding site (GESGSGKT) (exon 5) (*23*) and two putative actin binding sites (exon 15 and 19) (*24*). Two IQ motifs adjacent to the motor domain are encoded in exon 22 (*25*). The tail region of MYO15 contains a myosin tail homology 4 (MyTH4) domain (*26*), encoded in exons 27 and 28, similar to those present in unconventional myosins of *Acanthamoeba* (Myo4), *Caenorhabditis elegans* (Myo12/HUM-4 and HUM-6), *Bos taurus* (Myo10), and human (MYO7A) (*27*). A talin-like sequence was also found in the MYO15 tail region spanning exons 42 to 47 (*26*).

Myosins are classified on the basis of sequence divergence of their motor domains. To date, 14 classes have been defined (*28*). In a ClustalW alignment with the motor domains of MYO15 and other myosins, the highest amino acid identity was 42% with C. *elegans* HUM-6 (GenBank accession number U80848) and 41% with MYO7A (GenBank accession number U39226) (*29*). The extent of sequence divergence of MYO15 motor domain from other reported myosins qualifies *MYO15* as a new branch of the myosin superfamily (myosin-XV) (*7*).

To search for *MYO15* mutations in the Bengkala kindred and the two unrelated consanguineous Indian families (M21 and I-1924), we amplified and sequenced the 50 identified *MYO15* exons and flanking intronic sequences from DNA of affected individuals (*30*). In each of the families, a single mutation was identified that cosegregates with deafness (Fig. 2, A and B) (*31*). These mutations were not found in 390 chromosomes from 95 unrelated Indians

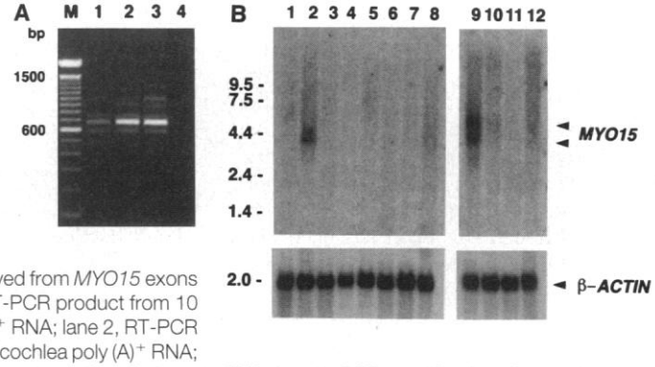

Fig. 3. Expression of *MYO15*. (**A**) Expression of *MYO15* in human fetal cochlea by RT-PCR analysis. RNA from human fetal cochlea and human placenta was reverse transcribed from an oligo(dT) primer and a portion of the first-strand cDNA was PCR amplified with primers derived from *MYO15* exons 21 and 27 (*37*). Lane 1, RT-PCR product from 10 ng of fetal cochlea poly (A)$^+$ RNA; lane 2, RT-PCR product from 20 ng of fetal cochlea poly (A)$^+$ RNA; lane 3, RT-PCR product from 1 μg of total placenta RNA; lane 4, PCR amplification of a mock reverse transcription reaction (no RNA). The primers will amplify a 688-bp product from cDNA and a 2903-bp product from genomic DNA. The identity of the 688-bp RT-PCR products from fetal cochlea and placenta was confirmed by sequence analysis. The PCR was run in a 1% agarose gel with 100-bp markers (lane M) (Gibco-BRL). (**B**) Northern blot analysis using a *MYO15* RT-PCR product from exons 29 to 47 as a probe. Each lane contains approximately 2 μg of poly (A)$^+$ RNA from a human adult (left, lanes 1 to 8) or from fetal tissue (right, lanes 9 to 12) (MTN blots 7760-1 and 7756-1; Clontech Laboratories). Lane 1, heart; lane 2, brain; lane 3, placenta; lane 4, lung; lane 5, liver; lane 6, muscle; lane 7, kidney; lane 8, pancreas; lane 9, brain; lane 10, lung; lane 11, liver; lane 12, kidney. The most intense hybridization signals (4.2 to 5.5 kb) were observed in poly (A)$^+$ RNA from adult and fetal brains (lanes 2 and 9). The same filters were rehybridized to a β-actin control probe for assessment of equal poly (A)$^+$ RNA loading and transfer efficiency and are shown in the lower panel. Hybridization conditions are described in (*13*).

and 100 unrelated Caucasians (*31*). In the Bengkala kindred, an A-to-T transversion (2674 A → T) in codon 892 (exon 28) is predicted to result in an Ile-to-Phe (I892F) substitution at a conserved position within the MyTH4 domain. The mutation identified in Indian family M21 (2668 A → T, exon 28) also is predicted to result in a substitution within the MyTH4 domain (Asp-to-Tyr; N890Y) and is found just two codons upstream of the mutation in the Bengkala families. Although a function for a MyTH4 domain is not known, the presence of these mutations suggests a critical role of this region of MYO15 in sensory transduction within the human inner ear. In contrast to these two missense mutations, the mutation identified in the other Indian family (I-1924) is a nonsense mutation in exon 39 (3898 A → T; K1300X) and is predicted to result in either a truncated protein or no protein at all (*32*).

MYO15 is expressed in human fetal and adult brain as evaluated by Northern blot analysis (Fig. 3B). As shown by dot-blot analysis of poly $(A)^+$ RNA from a variety of tissues, *MYO15* is expressed in ovary, testis, kidney, and pituitary gland (*33*, *34*). We also observed expression of *MYO15* by RT-PCR of poly $(A)^+$ RNA from cochlea of 18- to 22-week fetuses (Fig. 3A). Sequencing of the RT-PCR product confirmed that it corresponds to *MYO15*.

Our data show that *MYO15* may be expressed in a number of tissues in addition to the inner ear. However, there is no obvious consistent clinical abnormality other than profound deafness in affected individuals from these three *DFNB3* families. A possible explanation for the absence of pleiotropy of these *MYO15* mutations is the presence of functional redundancy provided by unconventional myosins expressed in other tissues. Alternatively, the region where the three *DFNB3* mutations occurred may be functionally significant only in the auditory system. The isoform of *MYO15* in the inner ear identified by RT-PCR does not contain exon 24, although this exon has been observed in cDNA clones derived from other tissues (*35*). Exon 24 contains translation stop codons in all three reading frames. Therefore, *DFNB3* missense and nonsense mutations in exons 28 and 39 are not likely to have a functional consequence for *MYO15* isoforms that include exon 24.

We have identified three mutations of *MYO15* in two geographically and ethnically diverse populations and are now in a position to evaluate the contribution of *DFNB3* to hereditary deafness worldwide. Additionally, our findings demonstrate that *MYO15* encodes an essential mechanoenzyme of the auditory system. Mutations in two other unconventional myosins, Myo6 and MYO7A, also cause hereditary deafness (*4*, *36*). This implies that unconventional myosins play crucial and nonredundant roles in auditory hair cell function. The discovery of *MYO15* provides another entry point toward an integrated understanding of auditory signaling pathways.

REFERENCES AND NOTES

1. W. E. Nance and A. Sweeney, *Otolaryngol. Clin. North Am.* **8**, 19 (1975).
2. G. Van Camp and R. J. H. Smith, *Hereditary Hearing Loss Homepage* (January 1998). Available at http://dnalab-www.uia.ac.be/dnalab/hhh/.
3. D. P. Kelsell *et al.*, *Nature* **387**, 80 (1997); X. C. Li *et al.*, *Nature Genet.* **18**, 215 (1998).
4. X-Z. Liu *et al.*, *Nature Genet.* **16**, 188 (1997); D. Weil *et al.*, *ibid.*, p. 191.
5. T. B. Friedman *et al.*, *ibid.* **9**, 86 (1995).
6. Y. Liang *et al.*, *Am. J. Hum. Genet.* **62**, 904 (1998).
7. F. J. Probst *et al.*, *Science* **280**, 1444 (1998).
8. M. A. Titus, *Trends Cell Biol.* **7**, 119 (1997); J. R. Sellers, H. V. Goodson, F. Wang, *J. Muscle Res. Cell Motil.* **17**, 7 (1996); R. E. Cheney and M. S. Mooseker, *Curr. Opin. Cell Biol.* **4**, 27 (1992); M. S. Mooseker and R. E. Cheney, *Annu. Rev. Cell Dev. Biol.* **11**, 633 (1995).
9. *Myo15* and *MYO15* gene symbols were approved by the HUGO/GDB Nomenclature Committee.
10. Human participation was approved by the Institutional Review Boards of National Institute of Neurological Disorders and Stroke/National Institute on Deafness and Other Communicative Disorders (OH97-DC-N006 and OH93-DC-016), Brigham and Women's Hospital (87-02294), Udayana University, Denpasar Bali (1997-1), and the All India Institute of Medical Genetics (S-8066-01).
11. Twenty-seven primer pairs were synthesized based on the sequence of predicted mouse *Myo15* exons. Only four primer pairs from exons 11, 14, 16, and 18 amplified human genomic DNA.
12. The 5′ and 3′ RACE reactions were performed with human fetal brain and placenta Marathon-Ready cDNAs (7402-1 and 7411-1; Clontech Laboratories).
13. A human chromosome 17 cosmid arrayed library was hybridized overnight at 42°C with 2×10^7 cpm of α-^{32}P-labeled *MYO15* cDNA fragment from exon 11 in Hybrisol I (Oncor). Filters were washed in 0.015 M NaCl containing 0.0015 M sodium citrate and 0.5% SDS at 55°C for 1 hour and autoradiographed. Northern blot analysis used the same hybridization conditions as above except that final washes were done at 65°C. Random fragments of cosmid 155d02 were subcloned and sequenced; 868 M13 sequence reads on PE/ABI 377s gave an average of 10-fold coverage of this cosmid [R. K. Wilson and E. R. Mardis, *Analyzing DNA*, B. Birren, E. D. Green, S. Klapholz, R. M. Myers, J. Roskams, Eds. (Cold Spring Harbor Laboratory Press, Cold Spring Harbor, NY, 1997), p. 398]. Contig assembly and editing were done with the Phred/Phrap/Consed suite of programs [B. Ewing, L. Hillier, M. C. Wendl, P. Green, *Genome Res.* **8**, 175 (1998); D. Gordon *et al.*, *ibid.*, p. 195 (available at http://www.genome.washington.edu/UWGC/)].
14. C. Burge and S. Karlin, *J. Mol. Biol.* **268**, 78 (1997). GRAIL and GENSCAN gene structure prediction programs are available at http://compbio.ornl.gov/Grail-bin/EmptyGrailForm and http://gnomic.stanford.edu/GENSCANW.html.
15. S. F. Altschul *et al.*, *Nucleic Acids Res.* **25**, 3389 (1997).
16. Human cosmid and mouse BAC sequences were compared [J. Pustell and F. C. Kafatos, *ibid.* **12**, 643 (1984)].
17. *MYO15* cDNA fragments were subcloned into pGEM T-Easy (Promega) and sequenced on a PE/ABI 377 using Thermo Sequenase dye terminators (Amersham Life Science).
18. Mouse *Myo15* has a predicted mini exon 6 with conserved amino acids and donor and acceptor splice sites. We have not yet identified this mini exon in *Myo15* cDNA clones.
19. Abbreviations for amino acid residues are as follows: A, Ala; C, Cys; D, Asp; E, Glu; F, Phe; G, Gly; H, His; I, Ile; K, Lys; L, Leu; M, Met; N, Asn; P, Pro; Q, Gln; R, Arg; S, Ser; T, Thr; V, Val; W, Trp; and Y, Tyr.
20. A. Wang, data not shown.
21. No *MYO15* expressed sequence tags (ESTs) were identified in dbEST and TIGR databases and *MYO15* clones were not present among 235,392 I.M.A.G.E. Consortium cDNAs (Genome Systems). The following are the top three P(N) scores obtained by a BLASTX search of GenBank with the *MYO15* cDNA sequence: *MYO7A* (accession number U39226), 1.3e-182; *Myo7A* (accession number U81453), 1.3e-177; *C. elegans* HUM-6 (accession number U80848), 6.2e-177.
22. D. F. Feng and R. F. Doolittle, *J. Mol. Evol.* **25**, 351 (1987).
23. A search of PROSITE reveals another potential ATP-guanosine triphosphate (GTP) binding site in exon 18. Available at http://www.ebi.ac.uk/searches/prosite_input.html.
24. H. M. Warrick and J. A. Spudich, *Annu. Rev. Cell Biol.* **3**, 379 (1987); J. A. Porter and C. Montell, *J. Cell Biol.* **122**, 601 (1993).
25. E. M. Espreafico *et al.*, *J. Cell Biol.* **119**, 1541 (1992); A. Houdusse, M. Silver, Ç. Cohen, *Structure* **4**, 1476 (1996).
26. A gapped BLASTP (*15*) search of the tail region of MYO15 (exons 23 and 25 to 50) gave statistically significant alignments to both of the two MyTH4 domains and the first talin-like domain of MYO7A (GenBank accession numbers U55208 and U39226). The bit score and *E* value of MYO15 to the first MyTH4 and talin-like domains of MYO7A are 59.7, 4e-09 and 43.4, 8e-04, respectively. The bit score and *E* value to the second MyTH4 domain are 48 and 1e-05.
27. Z-Y. Chen *et al.*, *Genomics* **36**, 440 (1996); J. P. Baker and M. A. Titus, *J. Mol. Biol.* **272**, 523 (1997).
28. V. Mermall, P. L. Plost, M. S. Mooseker, *Science* **279**, 527 (1998).
29. *MYO1C*, an unconventional myosin that maps to 17p13, was suggested as a *DFNB3* candidate [F. Crozet *et al.*, *Genomics* **40**, 332 (1997); T. Hasson *et al.*, *ibid.* **36**, 431 (1996)]. There is 37% amino acid identity between MYO1C and MYO15 in the motor domain.
30. Primer pairs to each *MYO15* exon were designed to amplify both the exon and 20 to 100 bp of flanking intronic sequence. Genomic DNA from affected individuals in three *DFNB3* families and normal controls were used as a template for PCR amplification. Sequences of these 50 primer pairs and the PCR amplification conditions can be obtained from the authors. PCR products were gel purified (Qiagen) and sequenced with Thermo Sequenase radiolabeled terminators (Amersham Life Science).
31. Both normal allele and mutant allele specific primers (ASO) were synthesized for the Bengkala and M21 families. Normal ASO (N-ASO) are 5′-GAACATCT-TCGGGAACTACA-3′ (Bengkala) and 5′-CGG-GAGAACATCTTCGGGA-3′ (M21). Mutant ASO (M-ASO) are the same as above except that the most 3′ nucleotide is T instead of A. The antisense primer is 5′-TTGGGCTCCACTGCTGGT-3′. PCRs were done in 25 μl using 1 unit of Taq DNA polymerase with each primer at 0.4 μM; 200 μM each deoxyadenosine triphosphate (dATP), deoxythymidine triphosphate (dTTP), deoxyguanosine triphosphate (dGTP), and deoxycytidine triphosphate (dCTP); and PCR buffer [10 mM tris-HCl (pH 9.0), 50 mM KCl_2, 1.5 mM $MgCl_2$, 0.1% Triton X-100] in a cycle condition of 94°C for 1 min and then 32 cycles of 94°C for 30 s, annealing temperature (53°C for Bengkala N-ASO and M-ASO, 59°C for M21 N-ASO and M-ASO) for 30 s, and 72°C for 30 s followed by 72°C for 6 min. For cosegregation analysis, genomic DNA from all available affected individuals and their family members was used for PCR amplification. PCR conditions for screening random individuals are the same as above. The mutation in family I-1924 removes an Xmn I site and thus restriction fragment length polymorphism (RFLP) analysis was used to screen the family and

random individuals. The primer pair used for genomic DNA amplification is 5′-TCTCCCTGGATTCTCATTTA-3′ (forward) and 5′-TCTTTGTCTTCTGTTCCACC-3′ (reverse). Reactions were performed in 25 μl using 1 unit of Taq DNA polymerase with each primer at 0.4 μM; 200 μM each dATP, dTTP, dGTP, and dCTP; and PCR buffer [10 mM tris-HCl (pH 8.3), 50 mM KCl_2,1.5 mM $MgCl_2$] in a cycle condition of 94°C for 1 min and then 35 cycles of 94°C for 30 s, 55°C for 30 s, and 72°C for 30 s followed by 72°C for 6 min. PCR products were purified (Qiagen), digested with Xmn I, and separated in a 2% agarose gel.

32. A nonsense mutation may affect mRNA stability and result in degradation of the transcript [L. Maquat, *Am. J. Hum. Genet.* **59**, 279 (1996)].
33. Data not shown; a dot blot with poly $(A)^+$ RNA from 50 human tissues (The Human RNA Master Blot, 7770-1, Clontech Laboratories) was hybridized with a probe from exons 29 to 47 of *MYO15* using the same condition as Northern blot analysis (*13*).
34. Smith–Magenis syndrome (SMS) is due to deletions of 17p11.2 of various sizes, the smallest of which includes *MYO15* and perhaps 20 other genes [(*6*); K-S Chen, L. Potocki, J. R. Lupski, *MRDD Res. Rev.* **2**, 122 (1996)]. *MYO15* expression is easily detected in the pituitary gland (data not shown). Haploinsufficiency for *MYO15* may explain a portion of the SMS phenotype such as short stature. Moreover, a few SMS patients have sensorineural hearing loss, possibly because of a point mutation in *MYO15* in trans to the SMS 17p11.2 deletion.
35. R. A. Fridell, data not shown.
36. K. B. Avraham *et al.*, *Nature Genet.* **11**, 369 (1995); X-Z. Liu *et al.*, *ibid.* **17**, 268 (1997); F. Gibson *et al.*, *Nature* **374**, 62 (1995); D. Weil *et al.*, *ibid.*, p. 60.
37. RNA was extracted from cochlea (membranous labyrinths) obtained from human fetuses at 18 to 22 weeks of development in accordance with guidelines established by the Human Research Committee at the Brigham and Women's Hospital. Only samples without evidence of degradation were pooled for poly $(A)^+$ selection over oligo(dT) columns. First-strand cDNA was prepared using an Advantage RT-for-PCR kit (Clontech Laboratories). A portion of the first-strand cDNA (4%) was amplified by PCR with Advantage cDNA polymerase mix (Clontech Laboratories) using human *MYO15*-specific oligonucleotide primers (forward, 5′-GCATGACCTGCCGGCTAATGGG-3′; reverse, 5′-CTCACGGCTTCTGCATGGTGCTCGGCTGGC-3′). Cycling conditions were 40 s at 94°C; 40 s at 66°C (3 cycles), 60°C (5 cycles), and 55°C (29 cycles); and 45 s at 68°C. PCR products were visualized by ethidium bromide staining after fractionation in a 1% agarose gel. A 688-bp PCR product is expected from amplification of the human *MYO15* cDNA. Amplification of human genomic DNA with this primer pair would result in a 2903-bp fragment.
38. We are grateful to the people of Bengkala, Bali, and the two families from India. We thank J. R. Lupski and K.-S. Chen for providing the human chromosome 17 cosmid library. For technical and computational assistance, we thank N. Dietrich, M. Fergusson, A. Gupta, E. Sorbello, R. Torkzadeh, C. Varner, M. Walker, G. Bouffard, and S. Beckstrom-Sternberg (National Institutes of Health Intramural Sequencing Center). We thank J. T. Hinnant, I. N. Arhya, and S. Winata for assistance in Bali, and T. Barber, S. Sullivan, E. Green, D. Drayna, and J. Battey for helpful comments on this manuscript. Supported by the National Institute on Deafness and Other Communication Disorders (NIDCD) (Z01 DC 00035-01 and Z01 DC 00038-01 to T.B.F. and E.R.W. and R01 DC 03402 to C.C.M.), the National Institute of Child Health and Human Development (R01 HD30428 to S.A.C.) and a National Science Foundation Graduate Research Fellowship to F.J.P. This paper is dedicated to J. B. Snow Jr. on his retirement as the Director of the NIDCD.

9 March 1998; accepted 17 April 1998

Continuity in Evolution: On the Nature of Transitions

Walter Fontana and Peter Schuster

To distinguish continuous from discontinuous evolutionary change, a relation of nearness between phenotypes is needed. Such a relation is based on the probability of one phenotype being accessible from another through changes in the genotype. This nearness relation is exemplified by calculating the shape neighborhood of a transfer RNA secondary structure and provides a characterization of discontinuous shape transformations in RNA. The simulation of replicating and mutating RNA populations under selection shows that sudden adaptive progress coincides mostly, but not always, with discontinuous shape transformations. The nature of these transformations illuminates the key role of neutral genetic drift in their realization.

A much-debated issue in evolutionary biology concerns the extent to which the history of life has proceeded gradually or has been punctuated by discontinuous transitions at the level of phenotypes (*1*). Our goal is to make the notion of a discontinuous transition more precise and to understand how it arises in a model of evolutionary adaptation.

We focus on the narrow domain of RNA secondary structure, which is currently the simplest computationally tractable, yet realistic phenotype (*2*). This choice enables the definition and exploration of concepts that may prove useful in a wider context. RNA secondary structures represent a coarse level of analysis compared with the three-dimensional structure at atomic resolution. Yet, secondary structures are empirically well defined and obtain their biophysical and biochemical importance from being a scaffold for the tertiary structure. For the sake of brevity, we shall refer to secondary structures as "shapes." RNA combines in a single molecule both genotype (replicatable sequence) and phenotype (selectable shape), making it ideally suited for in vitro evolution experiments (*3*, *4*).

To generate evolutionary histories, we used a stochastic continuous time model of an RNA population replicating and mutating in a capacity-constrained flow reactor under selection (*5*, *6*). In the laboratory, a goal might be to find an RNA aptamer binding specifically to a molecule (*4*). Although in the experiment the evolutionary end product was unknown, we thought of its shape as being specified implicitly by the imposed selection criterion. Because our intent is to study evolutionary histories rather than end products, we defined a target shape in advance and assumed the replication rate of a sequence to be a function of the similarity between its shape and the target. An actual situation may involve more than one best shape, but this does not affect our conclusions.

An instance representing in its qualitative features all the simulations we performed is shown in Fig. 1A. Starting with identical sequences folding into a random shape, the simulation was stopped when the population became dominated by the target, here a canonical tRNA shape. The black curve traces the average distance to the target (inversely related to fitness) in the population against time. Aside from a short initial phase, the entire history is dominated by steps, that is, flat periods of no apparent adaptive progress, interrupted by sudden approaches toward the target structure (*7*). However, the dominant shapes in the population not only change at these marked events but undergo several fitness-neutral transformations during the periods of no apparent progress. Although discontinuities in the fitness trace are evident, it is entirely unclear when and on the basis of what the series of successive phenotypes itself can be called continuous or discontinuous.

A set of entities is organized into a (topological) space by assigning to each entity a system of neighborhoods. In the present case, there are two kinds of entities: sequences and shapes, which are related by a thermodynamic folding procedure. The set of possible sequences (of fixed length) is naturally organized into a space because point mutations induce a canonical neighborhood. The neighborhood of a sequence consists of all its one-error mutants. The problem is how to organize the set of possible shapes into a space. The issue arises because, in contrast to sequences, there are

Institut für Theoretische Chemie, Universität Wien, Währingerstrasse 17, A-1090 Wien, Austria, Santa Fe Institute, 1399 Hyde Park Road, Santa Fe, NM 87501, USA, and International Institute for Applied Systems Analysis (IIASA), A-2361 Laxenburg, Austria.